Accepted Manuscript

Multiplexed assessment of the surface density of DNA probes on DNA microarrays by Surface Plasmon Resonance Imaging

László Simon, Róbert E. Gyurcsányi

PII: S0003-2670(18)31141-3

DOI: 10.1016/j.aca.2018.09.048

Reference: ACA 236284

To appear in: *Analytica Chimica Acta*

Received Date: 8 August 2018

Revised Date: 13 September 2018

Accepted Date: 20 September 2018

Please cite this article as: L. Simon, R.E. Gyurcsányi, Multiplexed assessment of the surface density of DNA probes on DNA microarrays by Surface Plasmon Resonance Imaging, *Analytica Chimica Acta* (2018), doi: https://doi.org/10.1016/j.aca.2018.09.048.

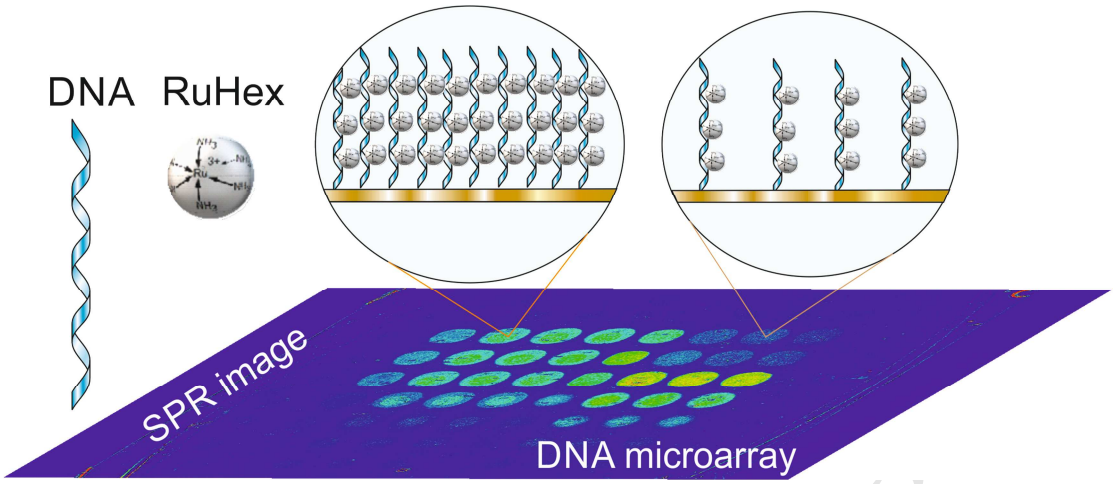

Multiplexed assessment of the surface density of DNA probes on DNA microarrays by Surface Plasmon Resonance Imaging

László Simon, Róbert E. Gyurcsányi*

Chemical Nanosensors Research Group, Department of Inorganic and Analytical Chemistry, Budapest University of Technology and Economics, Szent Gellért tér 4, H-1111 Budapest, Hungary

* corresponding author: Prof. Róbert E. Gyurcsányi (robertgy@mail.bme.hu)

Abstract

In terms of hybridization assays surface plasmon resonance imaging (SPRi) offers high throughput, label-free and real-time monitoring of the binding kinetics. This requires DNA microarrays on bare or modified gold SPRi chips, which are generally premade by an off-line microspotting procedure. Therefore, the surface density of the immobilized probes is not known although it is an essential quality control parameter, especially, when it can vary in a very broad range as in case of self-assembled thiol-labeled DNAs on gold surface. Here we show that the small molecular weight ruthenium(III) hexamine complex (RuHex) introduced earlier for electrochemical quantitation of DNA coverage on gold electrodes can be used also in SPRi to assess the surface density of DNA probes in DNA microarrays. A single injection of RuHex solution allows the simultaneous visualization and quantification of the surface density of DNA probes (ranging in this study from 4×10^{11} to 1.7×10^{13} molecules cm^{-2}) on all spots of a DNA microarray made by microspotting thiol labeled short DNA probes both in prehybridized and single-stranded form on a gold SPRi chip. The methodology was applied to determine the effect of the surface density of DNA probes on the hybridization efficiency and kinetics of complementary microRNAs, using hsa-miR-208a-3p as model. Single mismatch duplexes were found to be more effectively destabilized than fully complementary duplexes by steric hindrance at large surface densities of the DNA probes, which offers an effective mean to increase single mismatch selectivity.

Keywords: DNA surface density, microspotting, surface plasmon resonance imaging, DNA microarray, microRNA

1. Introduction

Surface plasmon resonance (SPR) is one of the gold standard methods for determining the kinetics and affinity of biomolecular interactions in a heterogeneous assay format. The limitations of the early two-channel systems in terms of sample throughput has been largely solved by the advent of SPR imaging (SPRi) [1, 2] that is able to assess simultaneously multiple interactions using microarray SPR chips. The label-free detection enabling real-time observation of the binding kinetics coupled with high throughput possibilities is clearly very appealing compared to conventional end-point detection based microarray technologies, e.g. fluorescence microarrays. Also in terms of analytical application a large number of signal amplification methods were reported by which the sensitivity of the SPR imaging (most often in the low nanomolar range) can be extended to approach that of fluorescence detection-based systems. Generally, nanoparticle and enzyme labeled probes (or their combination) are used to amplify the refractive index change in the sensing zone, either directly or by enzymatic deposition of a precipitate, respectively [3-6]. In case of nucleic acid microarrays the range of amplification schemes is even larger[7] by applying catalytic amplifications inherent to nucleic acid targets, e.g. polyadenylation[8] and RNAse H catalyzed hydrolysis[9] by which fM levels could be detected. To take advantage of the imaging methodology a large number of reactions partners needs to be immobilized in a site selective manner onto the surface of an SPR chip ensuring optimal binding of their targets. The latter is especially important for small molecular weight ligands such as peptides [10, 11] for which the molecular crowding on the surface may regulate also the molecular structure and function [12], as well as peptide nucleic acids [13] and DNA probes. In case of surface confined DNA probes the critical experimental parameters to be considered for proper hybridization efficiency are well known, e.g., surface density of probes [14-17], probe design [18], the type and length of spacers [19], the nanostructure of the surface [20, 21], ionic strength [15]. However, the optimal deployment of nucleic acid probes is also dependent on the type of detection used in the assay that limits the interlope of optimized immobilization methods between the various platforms. In channel-multiplexed SPR systems [22] the immobilization is less complex as requires solely the injection of the relevant coupling agents and probes into the channels. However, also the level of multiplexing is significantly smaller compared to photolithography or methods based on the local delivery and

consequent immobilization of DNA probes (e.g., micro- and nanospotting, continuous flow microfluidics, electrospotting [23]). Given the spatial resolution of the SPRi systems, microspotting is probably the most convenient choice in terms of versatility and cost-effective fabrication of DNA microarrays for SPR imaging. However, despite the fact that this technique is very well matured for DNA microarray fabrication on various polymeric and glass substrates its use for patterning SPR chips[24-26] and in particular bare gold chips [27, 28] has been only marginally addressed. One essential shortcoming of spotting-based SPRi microarray fabrication is that the probes are immobilized off-line, out of the instrument and therefore the immobilization and consequently the amount of surface confined probes cannot be followed and determined as in conventional or channel-multiplexed SPR systems. This is an important quality control parameter that should be provided to ensure the reproducibility of the probe immobilization and to enable the correct interpretation of the binding kinetics. Here we provide a solution to this problem by revealing the surface density of DNA probes using their reaction with ruthenium (III) hexamine (RuHex). This positively charged complex bounds electrostatically [29] to the surface confined DNAs and at properly chosen conditions may fully compensate for the negative charges on the DNA as shown earlier for DNA modified gold electrodes by chronocoulometric measurements [30]. We are reporting comprehensive data on the microspotting of thiol labeled DNA probes directly onto bare gold SPR chips and their optimization for hybridization assays correlated with RuHex assisted imaging of the surface density. The excellent control over the surface density of microspotted DNA probes was explored to enhance the selectivity of the DNA layers and to obtain reliable kinetic data on the hybridization of microRNA targets.

2. Experimental

2.1. Chemicals

The 22-mer microRNA hsa-miR-208a-3p (c-*miRNA*: 5’ – AUAAGACGAGCAAAAAGCUUGU – 3’), the complementary 18-mer thiol labeled DNA probe (*DNA probe*: 3’ – *ThiC3* -TATTCTGCTCGTTTTTCG – 5’, where *ThiC3* is HS-n-propyl) and a single mismatch 22-mer RNA (*sm-RNA*: 5’ – AUAAGACGA*A*CAAAAAGCUUGU – 3’) were purchased from Sigma-Aldrich. The DNA and RNA stock solutions were prepared with RNAse-, and DNAse-free water for molecular

biology (Diethyl pyrocarbonate -treated and sterile filtered; Sigma) in DNA LoBind centrifuge tubes (Eppendorf). Hexaammineruthenium(III)chloride ($[Ru(NH_3)_6]^{3+}$, RuHex) as well as 6-mercapto-1-hexanol (MH) and deoxyribonucleic acid sodium salt from salmon testes (salmon sperm DNA) were from Sigma-Aldrich. All other reagents such as inorganic salts and buffer components were of highest bioanalytical grade and were purchased from Sigma. Aqueous solutions were prepared with ultrapure deionized water (18.2 MΩ cm resistivity, Millipore).

2.2. DNA microspotting

Bare gold SPR biochips (HORIBA Jobin Yvon S.A.S. Palaiseau, France) were cleaned immediately before microspotting by UV ozone treatment (Novascan Technologies, Ames, IA, USA) for 30 min. Thiol-labeled DNA probes were microspotted onto gold chips using a BioOdyssey™ Calligrapher™ miniarrayer (Bio-Rad, Hercules, CA, USA) with a 500 μm diameter SMP15 Stealth Micro Spotting Pin (Arrayit Corporation, San José, USA) having an uptake volume of 0.25 μL. The DNA probes were dissolved in PBS at different concentrations and 20 μL aliquots were placed in the wells of a 384 well microtiter plate (LD-PE, DNA LoBind, PCR clean, Eppendorf) from which were spotted onto the gold chip. Each probe concentration was spotted in triplicate at 65 rh% and with the spotting stage thermostated at 12°C. The microarrays were then incubated at 20±1°C and 65 rh% in the humidity chamber of the microspotter for 4 h. In these conditions the drying of the spotted droplets was avoided during surface modification and the droplets were still visible before the DNA chips were blocked with 1 mM MH in phosphate buffer saline (PBS) for 60 min. Finally, the chips were washed with 200 mL DI water and gently dried under N_2 stream.

2.3. SPRi measurements

A XelPleX SPRi system (HORIBA France S.A.S. Palaiseau, France) was used at fixed optimal angles (typically 3-6 angles) to measure the hybridization interactions between the spotted DNA probes and microRNA strands. The reflectivity response (refractive index sensitivity) over the whole chip surface was normalized by using 3 mg mL^{-1} sucrose solution. To determine the surface density of

microspotted DNA probes 200 µL of 50 µM RuHex in TRIS buffer (10 mM TRIS, 50 mM NaCl, pH adjusted to 7.4 with 1M HCl) was injected at 50 µL min^{-1}. The binding of microRNAs to the DNA probes was monitored upon injecting 500 µL target aliquots in PBS working buffer (10 mM phosphate, 137 mM NaCl, 2.7 mM KCl, pH 7.4) at 50 µL min^{-1}. Between consecutive target-probe interaction measurements the surface confined DNA probes were regenerated, i.e., the hybridized target strands were removed using alkaline dehybridization by flowing 200 µL of 100 mM NaOH solution for 4 min over the chip surface. All experiments were performed at 25° C and the solutions were injected from the wells of 96 deepwell LD-PE plates (DNA LoBind, PCR clean, Eppendorf) placed in the autosampler unit of the instrument. The kinetics of the interactions were determined with Scrubber 2 GenOptics version (BiaLogic Software, Campbell, Australia). The typical durations for recording the baseline, association and dissociation steps were 3, 10, and 23 min, respectively.

3. Results and discussion

3.1. Determination of the surface density of microspotted DNA probes

The thiol labeled DNA probes were microspotted on bare gold chips followed by a post treatment with MH to block the free gold surface and also to strip non-specifically adsorbed DNAs (adsorbed through nucleotides). While residual amount of non-specifically adsorbed DNA was reported to persist even after MH treatment[31] especially for short probes (<24-mer), as in our case, immobilization through terminal thiol groups is expected to largely prevail [32]. The DNA probes were microspotted in two forms, i.e., as single stranded (ssDNA) and in prehybridized (phDNA) form. The later implied the prehybridization of the probe with the complementary microRNA (c-miRNA), i.e. by premixing the solution of the respective nucleic acids with the c-miRNA in 10 percent molar excess. Before any further experiments the phDNA spots were activated by removing the bound c-miRNA strands using 100 mM NaOH as described in the experimental section.

We found in an earlier study aimed at preparation of PNA microarrays [13] that the activation of the probes microspotted in prehybridized form (removal of the complementary strand), enabled the quantitation of the PNA surface density in multiplexed manner by SPRi. Unfortunately, this methodology is not applicable for DNA probes due to the marked ionic strength dependence of DNA-

RNA duplexes as opposed to PNA-RNA. Thus, loss of c-miRNA case of DNA probes occurred during the successive washing steps applied after microspotting, in particular at rinsing with DI water. This loss prohibited the accurate assessment of the surface density of the probes during the regeneration step in the SPRi instrument. In principle, the amount of complementary strands bound at saturation in a subsequent hybridization reaction may also be used as a measure of the amount of DNA probes immobilized, however this amount is affected beside the surface density of the probe also by the hybridization efficiency, e.g., at high surface densities the steric and electrostatic repulsion may decrease the amount of the c-miRNA bound and that would cause a significant negative bias in the determined surface density.

To address this problem, we explored the use of RuHex as a small molecular weight cation that was shown in electrochemical studies to bind electrostatically and in properly chosen experimental conditions to quantitatively compensate the negative charge of surface confined DNA strands [30]. Our hypothesis was that due to its small size RuHex can penetrate even dense DNA layers inaccessible to complementary strands and cause detectable refractive index changes. Therefore, the proper ionic strength and RuHex concentrations in this respect were determined for the highest DNA probe surface density investigated in this study, which was achieved by microspotting 30 µM ssDNA. Figure 1A shows the result of the systematic optimization involving the change of the RuHex concentration and ionic strength through variation of the NaCl content of the 10 mM TRIS pH 7.4 working buffer. It was found that 50 µM RuHex and 50 mM NaCl provided the highest reflectivity change, which is indicative of the maximal amount of RuHex in the DNA layer (ca. 1.8×10^{13} molecules cm^{-2}). These experimental conditions were used in all subsequent measurements. While the optimal saturation value of the RuHex (Figure 1B) was found to be exactly the same as determined by Steel in their electrochemical DNA quantitation method [30], the ionic strength in this study is at least 5 times higher. However, as visible in Figure 1A a rather large tolerance is noticeable in terms of the ionic strength at the optimal RuHex concentration. Of note, RuHex is weakly bound by electrostatic interaction to surface confined DNA strands with association constants generally in the range of 10^5 and 10^6 M^{-1} DNA [29] depending on the experimental conditions. One important implication of the weak association is that the RuHex binding to surface confined DNA strands is fully reversible. This

is clearly supported by Figure 1 C showing that during association-dissociation cycles of RuHex for various surface density DNA probes a full recovery of the baseline is achieved already in the dissociation step. Given the weak interaction, RuHex binding throughout this paper is measured in the presence of a high excess of RuHex (50 µM) in the buffer solution to ensure the saturation of surface confined DNAs. As shown in Figure 1C, for the solely MH covered gold surface, the presence of RuHex in the working buffer does not cause any significant bulk refractive index change with respect of the RuHex-free buffer.

Figure 1.

To calculate the surface density of DNA probes it is assumed that the negative charge of the DNA layer is quantitatively compensated by the triply charged RuHex cation as thoroughly studied earlier [30]. Thus the surface density of DNA ($\Gamma_{\text{DNA probe}}$ in molecules cm^{-2}) can be expressed as:

$$\Gamma_{\text{DNA probe}} = \frac{\Gamma_{RuHex} \times N_{Av} \times 10^{-10}}{MW_{RuHex} \times \frac{N}{3}} \qquad \text{Eq.1}$$

where, $\Gamma_{RuHex}$is the surface excess of RuHex corresponding to complete charge compensation of the DNA layer, N_{Av} is the Avogadro constant; MW_{RuHex} is the molecular weight of RuHex (203.25 g mol^{-1}); N is the number of nucleotides in the DNA probe. To calculate the surface density of RuHex (pg mm^{-2}) the following expression was used [33]:

$$\Gamma_{RuHex} = \frac{R_{max_{RuHex}} \cdot L_{Z_C}}{\frac{\delta R}{\delta n} \cdot \frac{\delta n}{\delta c_m}} = \frac{R_{max_{RuHex}} \cdot L_{Z_C}}{\frac{\delta R}{\delta c_m}} \qquad \text{Eq.2}$$

where $R_{max_{RuHex}}$ is the change of reflectivity (%) at saturation, L_{ZC} is the penetration depth of the evanescent wave in the medium above the gold layer (1.75×10^{-4} mm for 810 nm laser used in XelPlex, as provided by the instrument manufacturer). $\delta R/\delta n$ and $\delta n/\delta c_m$ are the slopes of the linear relationships between the reflectivity change and refractive index ($\delta R/\delta n$= 9354 ± 65) as well as the refractive index change and the RuHex concentration ($\delta n/\delta c_m$= 1.857 ± 0.012 × 10^{-10} mm^3 pg^{-1}), respectively. After confirming the linearity of the respective relationships (Figure S1, SI) the reflectivity change as a function of the RuHex concentration ($\delta R/\delta c_m$= 1.775 ± 0.014 × 10^{-6} mm^3 pg^{-1})

is ultimately needed for the quantitation of the surface excess of RuHex. Thus a single injection of RuHex solution enables from the reflectivity changes measured (Eq. 1 and 2) the quantitative determination of the surface density of immobilized DNA probes for all spots of the DNA microarray. Since the RuHex binding is a fully reversible process the DNA bound RuHex can be simply removed by dissociation during flushing the cell with the working buffer. Thus, after the determination of the surface density of DNA probes the DNA microarray can be used further for hybridization assays without any additional regeneration.

Figure 2 shows differential SPR images of RuHex and c-miRNA binding to DNA microarrays prepared by microspotting various concentrations of thiol labeled ssDNA or phDNA onto bare gold surface. The RuHex injection was used to quantify the surface density of the immobilized DNA probe followed by injection of 100 nM complementary miRNA. The differential image obtained by subtracting the SPR image of the DNA microarray before the injection from that recorded after injection of RuHex or c-miRNA reveals the net effect (binding) of the respective compounds. The subtraction of the two SPR images involves the subtraction of the reflectivity values of the pixels with the same spatial coordinates for all pixels of the two images. Given the reversibility of RuHex binding, the SPR image after injection of RuHex was measured in the RuHex solution as described earlier. The results show that RuHex, despite of its low molecular weight it is a very sensitive mean to visualize the DNA microspots on SPRi chips revealing beside the quantitative assessment of their surface density also the homogeneity of the DNA spots.

Figure 2.

Further quantitative analysis of the surface density of DNA probes by SPRi is shown in Figure 3. The surface density of the ssDNA layers as determined from the amount of bound RuHex increased monotonously with the DNA concentration of the microspotted solution reaching close to saturation at 30 μM, which corresponds to a dense DNA layer of ca. $17.71 \pm 0.17 \times 10^{12}$ molecules cm^{-2} (Fig. 3A). However, such high surface densities of DNA probes are expected to have a negative effect on the efficiency of subsequent hybridization reactions. This was confirmed by determining the surface density of DNA probes also from the amount of c-miRNA hybridized to the various surface density DNA spots. First, for all the various concentration DNA spots c-miRNA calibrations were recorded

and the reflectivity change at saturation (R_{max}, Figure S2, SI) was used to determine the amount of c-miRNA bound and consequently to calculate the probe density assuming 1:1 interaction. The amount of hybridized c-miRNA goes through a maximum that corresponds to ca. 5 µM spotting concentration ($3.09 \pm 0.014 \times 10^{12}$ molecules cm^{-2}) and decreases practically to zero at spotting concentrations larger than 20 µM. Similarly poor hybridization efficiencies were observed for high probe densities on polycrystalline gold electrodes by electrochemical assessment [15] and the surface density corresponding to the maximal hybridization efficiency is agreement with theoretical predictions based on electrostatic DNA surface hybridization model [34]. As expected there is an optimal spotting concentration above which the hybridization becomes sterically hindered and ultimately completely suppressed upon formation of a "compact" DNA layer. In this region estimating the surface density of the probe from the hybridized complementary miRNA is completely misleading and prone to a large negative bias. Therefore, the results clearly show the utility of the RuHex–based DNA surface density assessment that appears to cover a large range of surface densities without being affected by steric hindrance.

When the DNA probe is microspotted in prehybridized form the maximal surface density ($5.95 \pm 0.04 \times 10^{12}$ molecules cm^{-2}) is reached at ca. 5 µM spotted probe concentration similar as in case of ssDNA spotting, however, it remains almost constant even if the spotted DNA concentration is further increased (Fig. 3B). Thus if the DNA probes are immobilized in prehybridized form the spacing effect of the complementary strand prohibits the formation of excessively high surface densities that would hinder the rebinding of the complementary strand, i.e., the surface density is self-regulated by immobilizing the DNA probe in prehybridized form. In practice this means that if such probes are immobilized from solutions with sufficiently high phDNA concentrations (in this case >5 µM) than the optimal hybridization efficiency can be achieved without any further optimization of the spotted probe concentration.

Figure 3.

Figure 3C shows that in terms of hybridization efficiency the very same performance can be achieved by both phDNA and ssDNA microspotting under optimized conditions. The amount of c-miRNA hybridized at spotting concentrations higher than 5 µM seem to be limited in case of phDNA spots

mainly by electrostatic repulsion given the self-regulating effect of the complementary microRNA that adjust the spacing between the immobilized probes, while in case of ssDNA additionally by steric repulsion. The electrostatic repulsion was confirmed by increasing the ionic strength of the working buffer that resulted in both cases in increasing amounts of hybridized c-miRNA (Figure S3, SI). However, the maximum type behavior of the probes immobilized in single stranded form was preserved even at higher ionic strength indicating steric hindrance at high surface densities. This was not the case for phDNA probes that preserved the saturation type response also at higher ionic strength.

3.2. Effect of the probe surface density on kinetic measurements and selectivity

For analytical applications the surface density of the DNA probe leading to the highest hybridization efficiency is preferred. However, it is well known that for determination of the kinetic and equilibrium constants lower probe surface densities that enable unhindered hybridization are preferred. Figure 4A shows the equilibrium dissociation constant (K_D) for the hybridization reaction for various surface densities of the DNA probes. For low spotting concentrations (<5 µM) the K_D values obtained for ssDNA and phDNA spots were within the experimental error the same (ca. 5.5 nM). However, at higher spotting concentrations a marked increase of the K_D values, up to ca. 22.5 nM, was observed for ssDNA layers. Analyzing the rate constants of the hybridization reaction (Figure S4, SI) revealed that this is mainly due to the increased dissociation rate constants as the ssDNA probe surface density increases while the association rate constants remain fairly constant. Of note, the fitting of the relevant kinetic curves was very accurate for all the different surface density spots with a detectable reflectivity change (Figure 4B). If the probes were spotted in prehybridized form the K_D values were practically independent of the spotted concentrations, which makes this approach particularly robust for K_D determination.

Figure 4.

Given the marked dependence of K_D on the probe surface density in case of ssDNA spotted surfaces we were further interested whether this effect can be exploited to increase the selectivity against single base mismatches. Thus various probe surface densities were established by microspotting

different concentration ssDNA and the amount of hybridized complementary microRNA and single base mismatch RNA (sm-RNA), with the mismatch located in the middle of the strand, was compared (Figure 5 A). For both RNAs a maximum in the binding efficiency was observed that occurred at a similar spotting concentration of ca. 5µM. More importantly, at this surface density corresponding to optimal hybridization efficiency the c-miRNA was only ca. 14 % higher than that of the sm-RNA strands, which might be insufficient for its reliable assessment in the presence of single mismatch strands. However, for sm-RNA binding a much steeper decrease of the hybridization efficiency was found with increasing surface density of the DNA probe. Thus for ca. 10 µM spotting concentration, corresponding to a surface density of ca. 5.33×10^{12} molecules cm^{-2}, the sm-RNA hybridization is effectively suppressed, while the c-miRNA binding is still detectable. This means that in case of larger surface density DNA probes that sterically hinders the hybridization, the single mismatched duplexes are destabilized more effectively than the fully complementary duplex. This is evidentiated also by the effect of the DNA surface density on the respective K_D values (Figure 5 B). Indeed, for the lowest surface density of the DNA probe (ca. 9.26×10^{11} molecules cm^{-2}) the K_D value of the complementary strand (5.9 nM) was smaller only with a factor of 2 than that of the sm-microRNA (11.6 nM). The gap however increased to more than a factor of 5 at 10 µM spotting concentration with a K_D of 62.7 nM for the sm-RNA and 11.47 nM for c-miRNA.

Figure 5.

Conclusions

A single injection of RuHex solution under optimized conditions as determined in this study is suitable to visualize microspotted thiol-labeled DNA probes on SPR chips and to estimate their surface density by SPRi. Since the RuHex binding is independent of the sequence of the immobilized DNA probes [30] and the resulted complex can be disrupted in mild conditions, the method is applicable to the simultaneous, nondestructive assessment of the surface density of DNA probes in all spots of a DNA microarray as well as for their regular control during repeated experiments. While the coulometric assessment requires electrochemical addressability of the DNA bound RuHex, the SPRi based method introduced here is expected to be applicable for a broader range of immobilization strategies, e.g., through polymeric matrices and biotin-avidin coupling. The method proposed here can

be applied on other SPR devices, with the penetration depth being the main instrument depending parameter, and seems fully consistent for short DNA probes as required for microRNA targets.

The study revealed that DNA probes microspotted in both single stranded and prehybridized form can ultimately provide the same hybridization efficiency. For high spot density DNA microarrays the prehybridization with a complementary strand may not be practical due to higher cost, but it contours as the most robust approach for (i) kinetic measurements, (ii) small spot density DNA microarrays and (iii) in case of surface morphologies or nanoscale confinements where reproducible hybridization efficiencies are otherwise difficult to achieve, e.g., nanopores [35]. Arrays with microspotted ssDNA strands require more elaborate optimization in terms of hybridization efficiency, however allows for fine tuning of the surface coverage for a better discrimination of single mismatch targets.

Acknowledgement

The work was supported by Lendület program of the Hungarian Academy of Sciences (LP2013-63/2013), VKSZ_14-1-2015-0004 of the National Research, Development and Innovation Office, ERA-Chemistry (2014, 61133; OTKA NN117637) and BME-Nanotechnology FIKP grant of EMMI (BME FIKP-NAT). The scientific support provided Horiba France SAS during this work is gratefully acknowledged.

References

[1] D. Piscevic, R. Lawall, M. Veith, M. Liley, Y. Okahata, W. Knoll, Oligonucleotide hybridization observed by surface plasmon optical techniques, Appl. Surf. Sci., 90 (1995) 425-436.

[2] C.E. Jordan, A.G. Frutos, A.J. Thiel, R.M. Corn, Surface Plasmon Resonance Imaging Measurements of DNA Hybridization Adsorption and Streptavidin/DNA Multilayer Formation at Chemically Modified Gold Surfaces, Anal Chem, 69 (1997) 4939-4947.

[3] F. Nakamura, M. Ito, A. Manna, K. Tamada, M. Hara, W. Knoll, Observation of hybridization on a DNA array by surface plasmon resonace imaging using Au nanoparticles, Jpn. J. Appl. Phys., Part 1, 45 (2006) 1026-1029.

[4] M. Ito, F. Nakamura, A. Baba, T. Kaoru, H. Ushijima, K.H.A. Lau, A. Manna, W. Knoll, Enhancement of surface plasmon resonance signals by gold nanoparticles on high-density DNA microarrays, J. Phys. Chem. C, 111 (2007) 11653-11662.

[5] K. Tamada, F. Nakamura, M. Ito, X. Li, A. Baba, SPR-based DNA Detection with Metal Nanoparticles, Plasmonics, 2 (2007) 185-191.

[6] G. Festag, T. Schüler, A. Steinbrück, A. Csáki, R. Möller, W. Fritzsche, Chip-based molecular diagnostics using metal nanoparticles, Expert Opin. Med. Diagn., 2 (2008) 813-828.

[7] J.B. Fasoli, R.M. Corn, Surface Enzyme Chemistries for Ultrasensitive Microarray Biosensing with SPR Imaging, Langmuir, 31 (2015) 9527-9536.

[8] S. Fang, H.J. Lee, A.W. Wark, R.M. Corn, Attomole Microarray Detection of MicroRNAs by Nanoparticle-Amplified SPR Imaging Measurements of Surface Polyadenylation Reactions, J. Am. Chem. Soc., 128 (2006) 14044-14046.

[9] T.T. Goodrich, H.J. Lee, R.M. Corn, Direct Detection of Genomic DNA by Enzymatically Amplified SPR Imaging Measurements of RNA Microarrays, J. Am. Chem. Soc., 126 (2004) 4086-4087.

[10] A. Gori, M. Cretich, R. Vanna, L. Sola, P. Gagni, G. Bruni, M. Liprino, F. Gramatica, S. Burastero, M. Chiari, Multiple epitope presentation and surface density control enabled by chemoselective immobilization lead to enhanced performance in IgE-binding fingerprinting on peptide microarrays, Anal. Chim. Acta, 983 (2017) 189-197.

[11] T. Shimomura, X. Han, A. Hata, T. Niidome, T. Mori, Y. Katayama, Optimization of Peptide Density on Microarray Surface for Quantitative Phosphoproteomics, Anal. Sci., 27 (2011) 13-17.

[12] S.J. White, S.D. Johnson, M.A. Sellick, A. Bronowska, P.G. Stockley, C. Wälti, The Influence of Two-Dimensional Organization on Peptide Conformation, Angew. Chem. Int. Ed., 54 (2014) 974-978.

[13] L. Simon, G. Lautner, R.E. Gyurcsányi, Reliable microspotting methodology for peptide-nucleic acid layers with high hybridization efficiency on gold SPR imaging chips, Anal. Methods, 7 (2015) 6077-6082.

[14] J.H. Watterson, P.A.E. Piunno, C.C. Wust, U.J. Krull, Effects of Oligonucleotide Immobilization Density on Selectivity of Quantitative Transduction of Hybridization of Immobilized DNA, Langmuir, 16 (2000) 4984-4992.

[15] P. Gong, R. Levicky, DNA surface hybridization regimes, Proc. Natl. Acad. Sci. U.S.A., 105 (2008) 5301-5306.

[16] A.W. Peterson, R.J. Heaton, R.M. Georgiadis, The effect of surface probe density on DNA hybridization, Nucleic Acids Res., 29 (2001) 5163-5168.

[17] T.M. Herne, M.J. Tarlov, Characterization of DNA Probes Immobilized on Gold Surfaces, J. Am. Chem. Soc., 119 (1997) 8916-8920.

[18] F. Nakamura, M. Hara, The length effect of probe DNA for hybridization Using DNA self-assembled monolayer, e-J. Surf. Sci. Nanotechnol., 3 (2005) 250-253.

[19] S.S. Mark, N. Sandhyarani, C. Zhu, C. Campagnolo, C.A. Batt, Dendrimer-functionalized self-assembled monolayers as a surface plasmon resonance sensor surface, Langmuir, 20 (2004) 6808-6817.

[20] B.J. Hong, S.J. Oh, T.O. Youn, S.H. Kwon, J.W. Park, Nanoscale-controlled spacing provides DNA microarrays with the SNP discrimination efficiency in solution phase, Langmuir, 21 (2005) 4257-4261.

[21] R. Gasparac, B.J. Taft, M.A. Lapierre-Devlin, A.D. Lazareck, J.M. Xu, S.O. Kelley, Ultrasensitive Electrocatalytic DNA Detection at Two- and Three-Dimensional Nanoelectrodes, J. Am. Chem. Soc., 126 (2004) 12270-12271.

[22] H.J. Lee, T.T. Goodrich, R.M. Corn, SPR imaging measurements of 1-D and 2-D DNA microarrays created from microfluidic channels on gold thin films, Anal Chem, 73 (2001) 5525-5531.

[23] P. Guedon, T. Livache, F. Martin, F. Lesbre, A. Roget, G. Bidan, Y. Levy, Characterization and Optimization of a Real-Time, Parallel, Label-Free, Polypyrrole-Based DNA Sensor by Surface Plasmon Resonance Imaging, Anal Chem, 72 (2000) 6003-6009.

[24] J.S. Shumaker-Parry, R. Aebersold, C.T. Campbell, Parallel, Quantitative Measurement of Protein Binding to a 120-Element Double-Stranded DNA Array in Real Time Using Surface Plasmon Resonance Microscopy, Anal Chem, 76 (2004) 2071-2082.

[25] J.S. Shumaker-Parry, M.H. Zareie, R. Aebersold, C.T. Campbell, Microspotting Streptavidin and Double-Stranded DNA Arrays on Gold for High-Throughput Studies of Protein-DNA Interactions by Surface Plasmon Resonance Microscopy, Anal Chem, 76 (2004) 918-929.

[26] N. Bassil, E. Maillart, M. Canva, Y. Lévy, M.-C. Millot, S. Pissard, R. Narwa, M. Goossens, One hundred spots parallel monitoring of DNA interactions by SPR imaging of polymer-functionalized surfaces applied to the detection of cystic fibrosis mutations, Sensor. Actuators. B Chem., 94 (2003) 313-323.

[27] L. Simon, G. Lautner, R.E. Gyurcsanyi, Reliable microspotting methodology for peptide-nucleic acid layers with high hybridization efficiency on gold SPR imaging chips, Analytical Methods, 7 (2015) 6077-6082.

[28] F. Pillet, C. Thibault, S. Bellon, E. Maillart, E. Trévisiol, C. Vieu, J.M. François, V.A. Leberre, Simple surface chemistry to immobilize DNA probes that significantly increases sensitivity and spots density of surface plasmon resonance imaging based microarray systems, Sensor. Actuators. B Chem., 147 (2010) 87-92.

[29] A.B. Steel, T.M. Herne, M.J. Tarlov, Electrostatic interactions of redox cations with surface-immobilized and solution DNA, Bioconjugate Chem., 10 (1999) 419-423.

[30] A.B. Steel, T.M. Herne, M.J. Tarlov, Electrochemical quantitation of DNA immobilized on gold, Anal Chem, 70 (1998) 4670-4677.

[31] M. Drozd, M.D. Pietrzak, E. Malinowska, SPRi-Based Biosensing Platforms for Detection of Specific DNA Sequences Using Thiolate and Dithiocarbamate Assemblies, Front. Chem., 6 (2018).

[32] A.B. Steel, R.L. Levicky, T.M. Herne, M.J. Tarlov, Immobilization of Nucleic Acids at Solid Surfaces: Effect of Oligonucleotide Length on Layer Assembly, Biophys. J., 79 (2000) 975-981.

[33] E. Bouffartigues, H. Leh, M. Anger-Leroy, S. Rimsky, M. Buckle, Rapid coupling of Surface Plasmon Resonance (SPR and SPRi) and ProteinChip™ based mass spectrometry for the identification of proteins in nucleoprotein interactions, Nucleic Acids Res., 35 (2007) e39-e39.

[34] I.Y. Wong, N.A. Melosh, An Electrostatic Model for DNA Surface Hybridization, Biophys. J., 98 (2010) 2954-2963.

[35] I. Makra, A. Brajnovits, G. Jágerszki, P. Fürjes, R.E. Gyurcsányi, Potentiometric sensing of nucleic acids using chemically modified nanopores, Nanoscale, 9 (2017) 739-747.

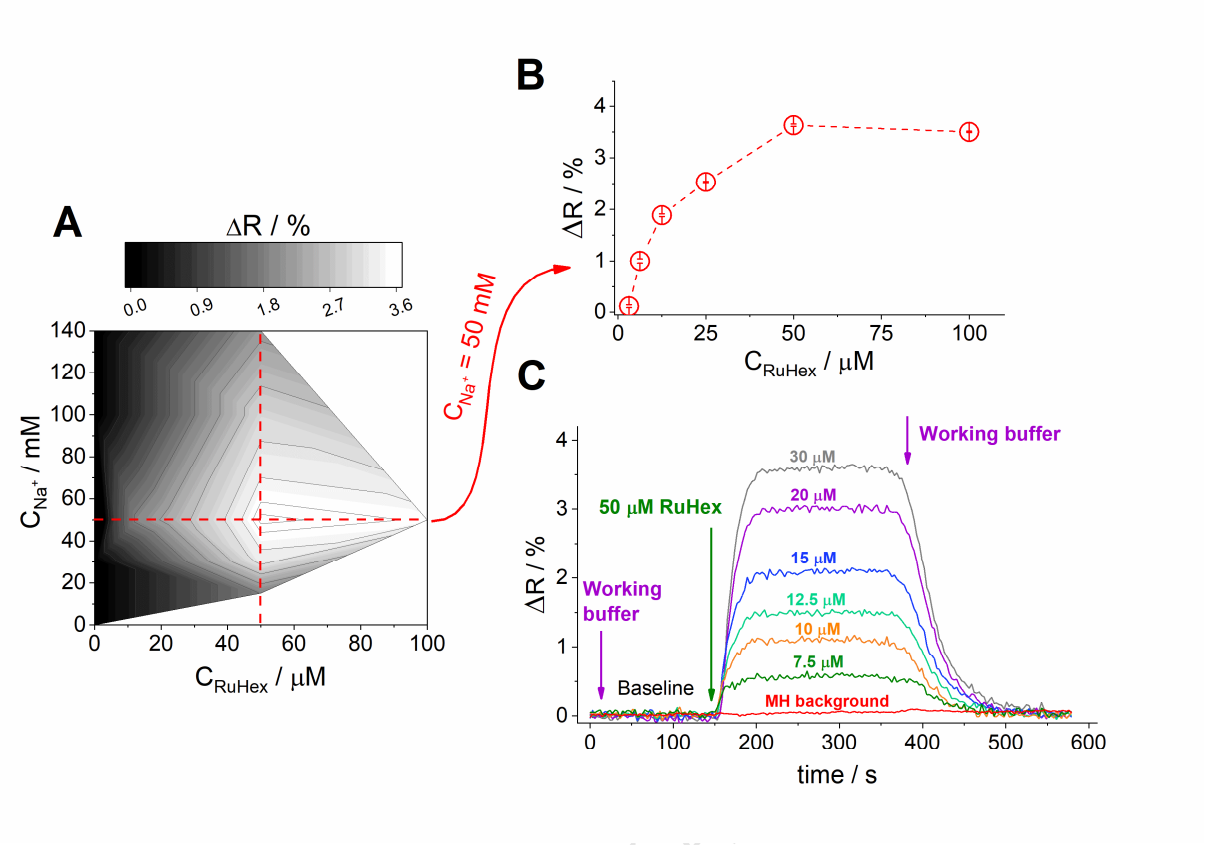

Figure 1. (A) Two-dimensional grayscale map of the reflectivity changes of DNA spots recorded upon injecting various concentration RuHex solution (horizontal axis) in different ionic strength working buffers (pH 7.4, 10 mM TRIS buffer) adjusted using different NaCl concentrations (vertical axis). The DNA probe was immobilized by spotting 30 μM thiol-labeled ssDNA on bare gold SPRi chip followed by blocking with MH. (B) RuHex adsorption isotherm for the optimal (50mM) NaCl concentration, the error bars are for 3 parallel spots on the same chip. (C) Reflectivity changes during association-dissociation cycles of RuHex to DNA probes microspotted at different concentration as indicated in the graph.

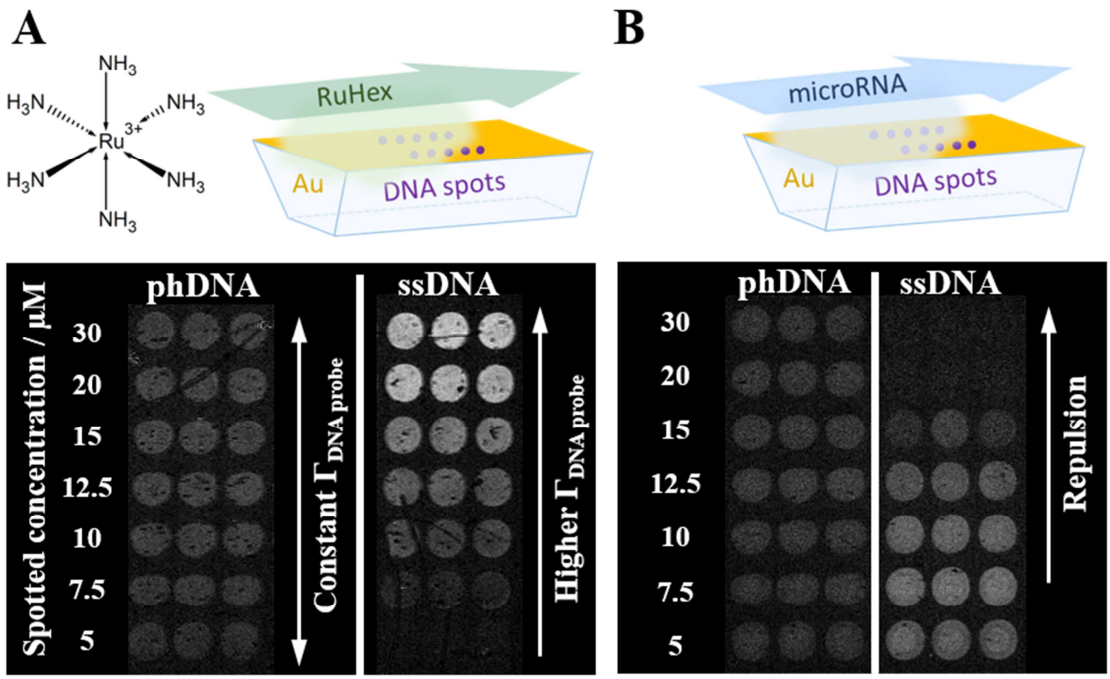

Figure 2. Differential SPR images of DNA microarrays microspotted in triplicate from various concentration DNA probe solutions (**A**) after injection of 50 µM RuHex and (**B**) after hybridization with 100 nM microRNA. The brightness of the spots scales with the amount of bound RuHex and microRNA, respectively.

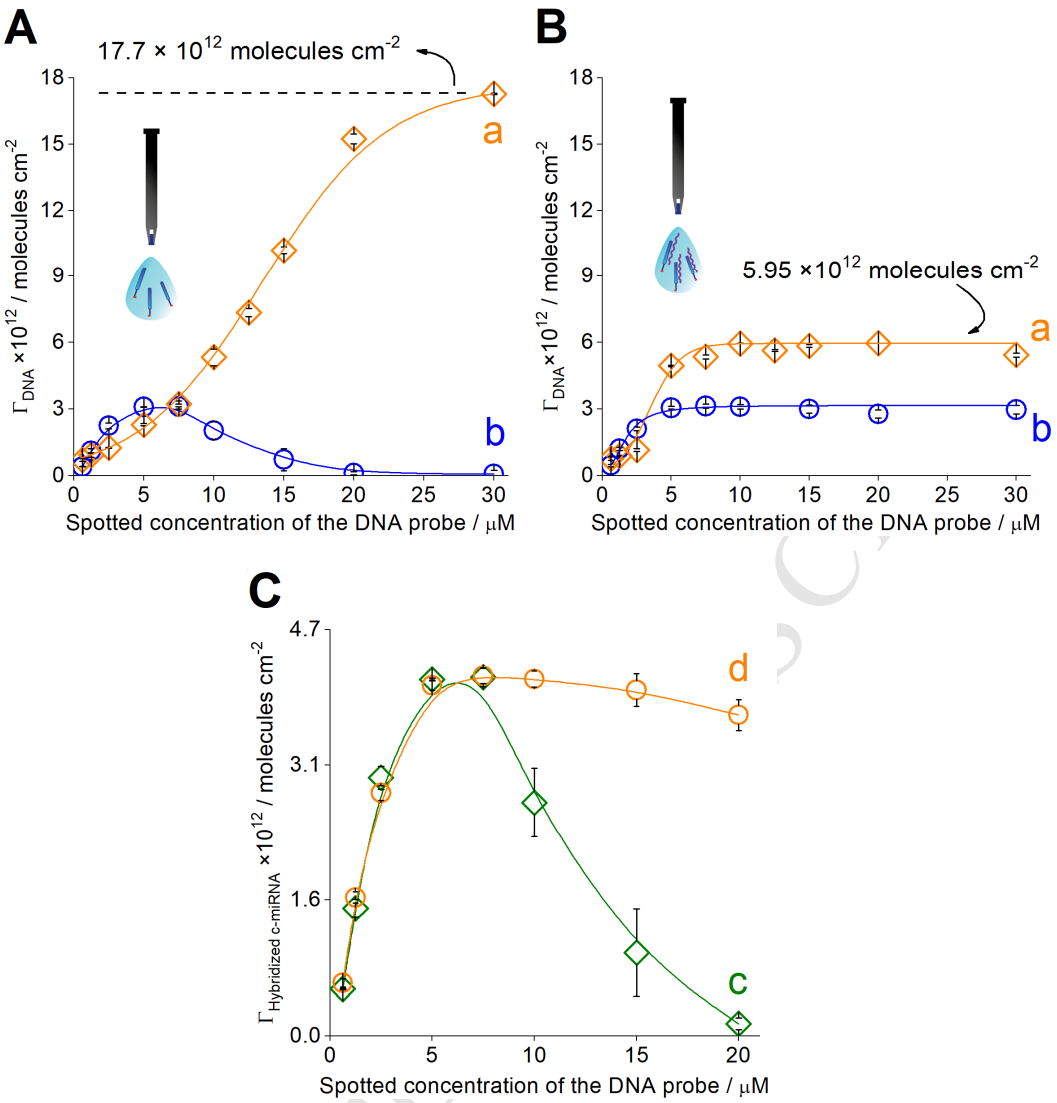

Figure 3. Surface density of the DNA probe as a function of the concentration of the microspotted thiol-labeled (**A**) ssDNA and (**B**) phDNA calculated from the amount of (**a**) RuHex bound (50 µM) and (**b**) hybridized c-miRNA. (**C**) Comparison of the amount of hybridized microRNA for ssDNA (**c**) and phDNA (**d**) microspots. Error bars are for 3 replicate spots on the same SPRi chip.

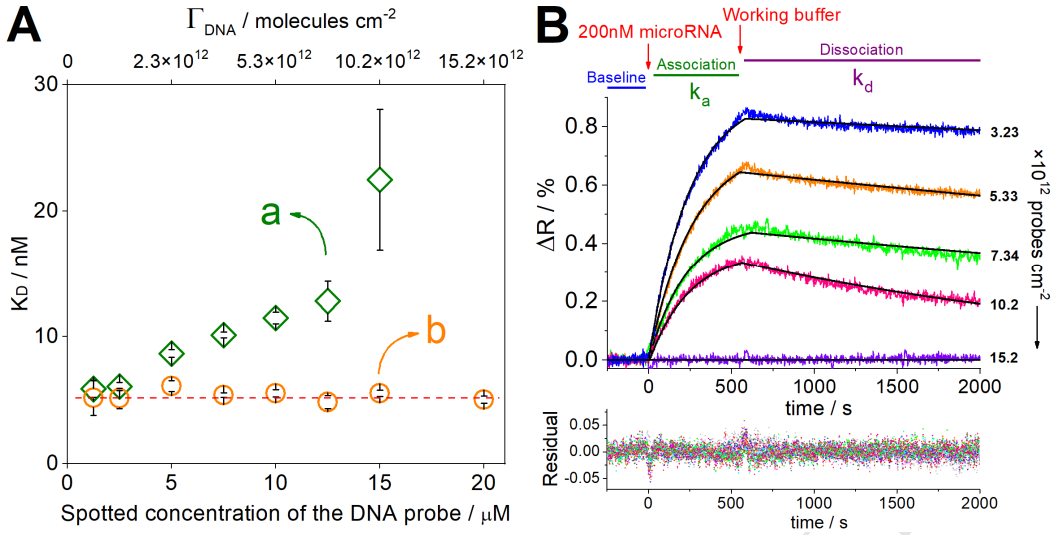

Figure 4. (**A**) Dissociation equilibrium constant as a function of the spotted DNA probe concentration in case of ssDNA (**a**) and phDNA (**b**). (**B**) Interaction plots upon injection of 200 nM c-miRNA for ssDNA spots with various surface probe concentration. Error bars are for 3 replicate spots on the same chip.

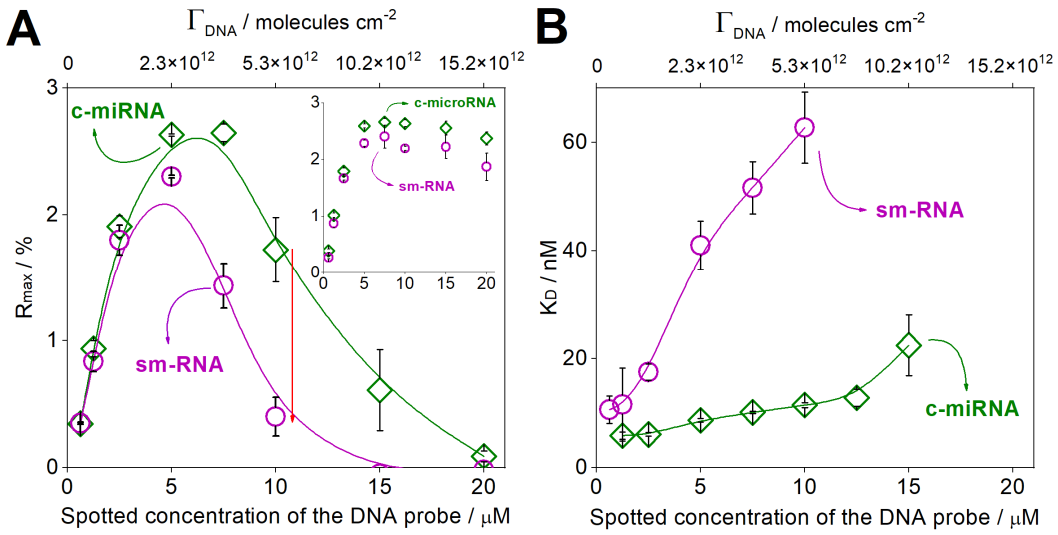

Figure 5. (**A**) Maximal reflectivity change of various surface density ssDNA spots (phDNA spots in the inset) in response to c-miRNA and sm-RNA as well as (**B**) the respective apparent equilibrium dissociation constants. Error bars are for 3 replicate spots on the same chip.

Highlights

- RuHex efficiently reveals immobilized DNA spots by SPRi on DNA microarrays
- Multiplexed quantitative assessment of DNA surface concentration is introduced
- The method enables convenient application-based optimization of DNA arrays
- DNA surface concentration is key to optimal selectivity and hybridization efficiency